The Cosmic Web:

Theory, Simulations, Observations, Reconstructions

Florent Leclercq

www.florent-leclercq.eu

Imperial Centre for Inference and Cosmology
Imperial College London

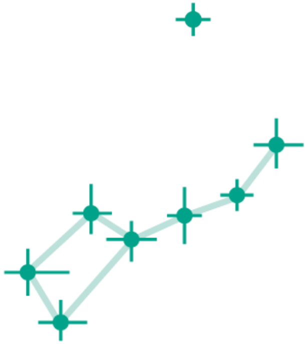

July 31st, 2019

Theory

Cosmic phase space: the Vlasov-Poisson system

- A self-gravitating fluid of cold dark matter (CDM):
  - Gravitational potential Φ:

Poisson equation: $\boxed{\Delta\Phi = 4\pi \mathrm{G} a^2 \bar{\rho}\delta}$ ⟵ Density contrast: $\delta(\mathbf{x},\tau) = \dfrac{\rho(\mathbf{x},\tau)}{\bar{\rho}} - 1$

  - Particle number density in phase space $f(\mathbf{x},\mathbf{p},\tau)$:

Vlasov equation: $$\boxed{\frac{\mathrm{d}f}{\mathrm{d}\tau} = \frac{\partial f}{\partial \tau} + \frac{\mathbf{p}}{ma}\cdot\nabla f - ma\nabla\Phi\cdot\frac{\partial f}{\partial p} = 0}$$

Collisionless version of the Boltzmann equation

- No hot component (apart from neutrinos):

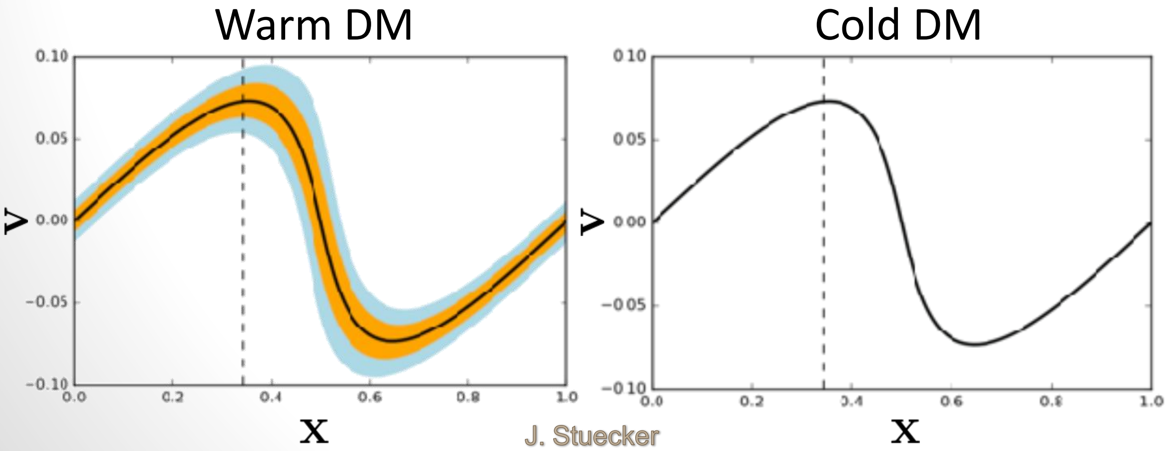
Warm DM

Cold DM

J. Stuecker

- Single-stream approximation:

$$f(\mathbf{x},\mathbf{p},\tau) = \rho(\mathbf{x},\tau)\,\delta_{\mathrm{D}}[\mathbf{p} - ma\mathbf{u}(\mathbf{x})]$$

Cosmic phase space: Lagrangian vs Eulerian views

- Consequence of the single-stream approximation:

$$\mathbf{x} = \mathbf{x}(\mathbf{q}, \tau)$$
$$\mathbf{v} = \mathbf{v}(\mathbf{q}, \tau)$$

$$\mathbf{x} = \mathbf{q} + \mathbf{\Psi}(\mathbf{q})$$

Lagrangian displacement field

Eulerian coordinate

Lagrangian coordinate

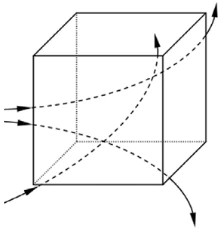

Spatially fixed volume element

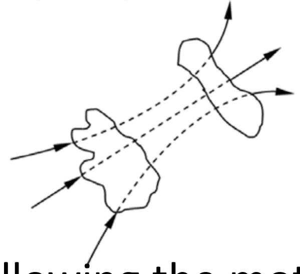

Following the motion of the fluid element

Eulerian coords

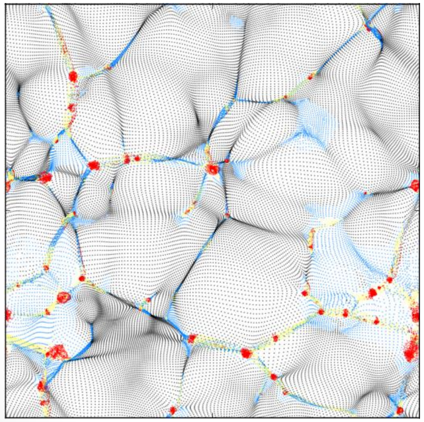

Lagrangian coords

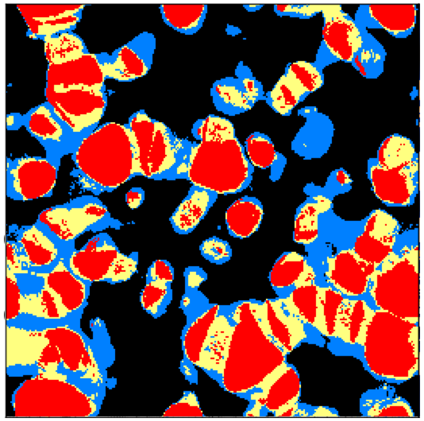

Neyrinck & Shandarin 2012, 1207.4501

Hydrodynamic models

- Momentum moments of the Vlasov equation:

$$\int f(\mathbf{x},\mathbf{p},\tau)\,\mathrm{d}^3\mathbf{p} \equiv \rho(\mathbf{x},\tau)$$

Density field

$$\int \frac{\mathbf{p}}{ma} f(\mathbf{x},\mathbf{p},\tau)\,\mathrm{d}^3\mathbf{p} \equiv \rho(\mathbf{x},\tau)\mathbf{u}(\mathbf{x},\tau)$$

Peculiar velocity flow

$$\int \frac{\mathbf{p}_i\mathbf{p}_j}{m^2a^2} f(\mathbf{x},\mathbf{p},\tau)\,\mathrm{d}^3\mathbf{p} \equiv \rho(\mathbf{x},\tau)\mathbf{u}_i(\mathbf{x},\tau)\mathbf{u}_j(\mathbf{x},\tau) + \sigma_{ij}(\mathbf{x},\tau)$$

$$\vdots$$

Stress tensor

Velocity dispersion tensor

$$\sigma_{ij}(\mathbf{x},\tau) = \rho(\mathbf{x},\tau)v_{ij}(\mathbf{x},\tau)$$

$$\vdots$$

Give hierarchy of conservation laws (0th: particle number, 1st: momentum, 2nd: energy, etc.)

- In the single-stream approximation: $\sigma_{ij} = 0$

$$\frac{\partial\delta(\mathbf{x},\tau)}{\partial\tau} + \nabla\cdot\{[1+\delta(\mathbf{x},\tau)]\,\mathbf{u}(\mathbf{x},\tau)\} = 0$$

conservation equation

$$\frac{\partial\mathbf{u}_i(\mathbf{x},\tau)}{\partial\tau} + \mathcal{H}(\tau)\mathbf{u}_i(\mathbf{x},\tau) + \mathbf{u}_j(\mathbf{x},\tau)\cdot\nabla_j\mathbf{u}_i(\mathbf{x},\tau) = -\nabla_i\Phi(\mathbf{x},\tau)$$

Euler equation

$$\Delta\Phi(\mathbf{x},\tau) = 4\pi\mathrm{G}a^2(\tau)\bar{\rho}(\tau)\delta(\mathbf{x},\tau)$$

Poisson equation

Still a heavily non-linear system!

Shell-crossing

- The breakdown of $\sigma_{ij} \approx 0$, describing the generation of velocity dispersion or anisotropic stress due to the multiple-stream regime, is generically known as shell-crossing.

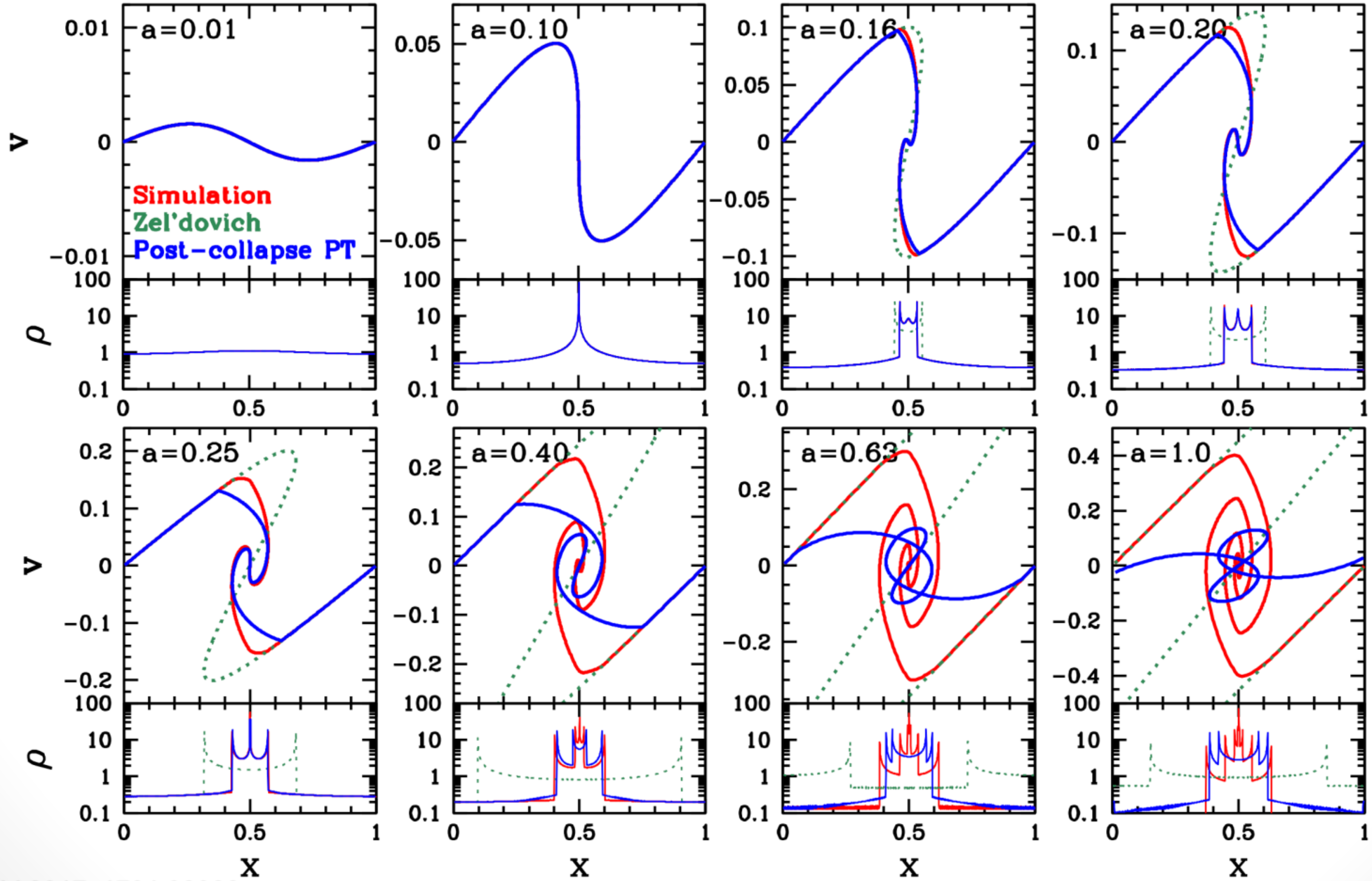

Taruya & Colombi 2017, 1701.09088

Simulations

Particle-mesh (PM) codes

- Equations of motion of particles:

$$\mathbf{p} = a\frac{\mathrm{d}\mathbf{x}}{\mathrm{d}\tau}$$

$$\frac{\mathrm{d}\mathbf{p}}{\mathrm{d}\tau} = -a\nabla\Phi$$

$$\Delta\Phi = 4\pi \mathrm{G} a^2 \bar{\rho}(\tau)\delta$$

$$\frac{\mathrm{d}\mathbf{x}}{\mathrm{d}a} = \mathcal{D}(a)\mathbf{p}$$

$$\frac{\mathrm{d}\mathbf{p}}{\mathrm{d}a} = \mathcal{K}(a)\nabla\left(\Delta^{-1}\delta\right)$$

“Drift” prefactor

“Kick” prefactor

- The Kick-Drift-Kick (leapfrog) integrator:

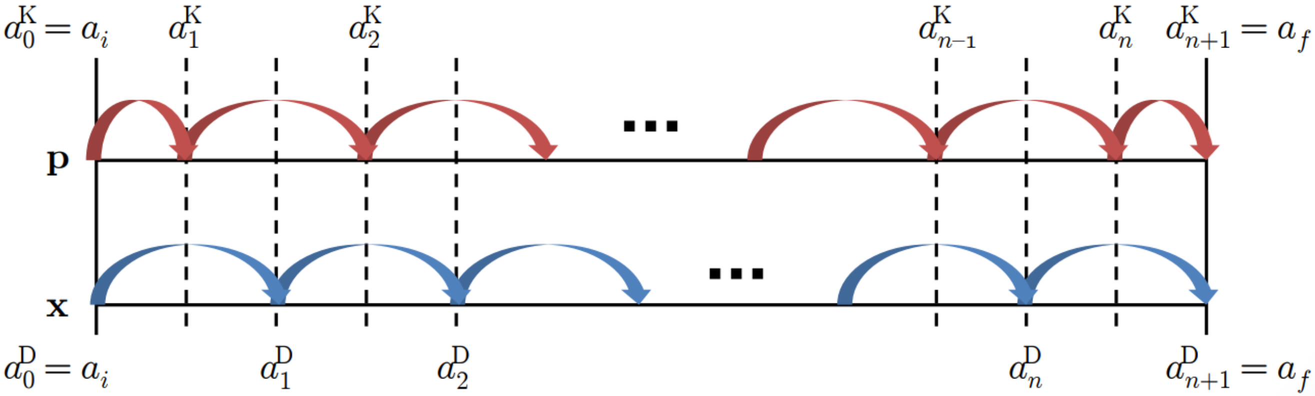

More extensive review in FL 2015, Appendix B, 1512.04985 or http://florent-leclercq.eu/documents/thesis/AppendixB.pdf

A dark matter simulation

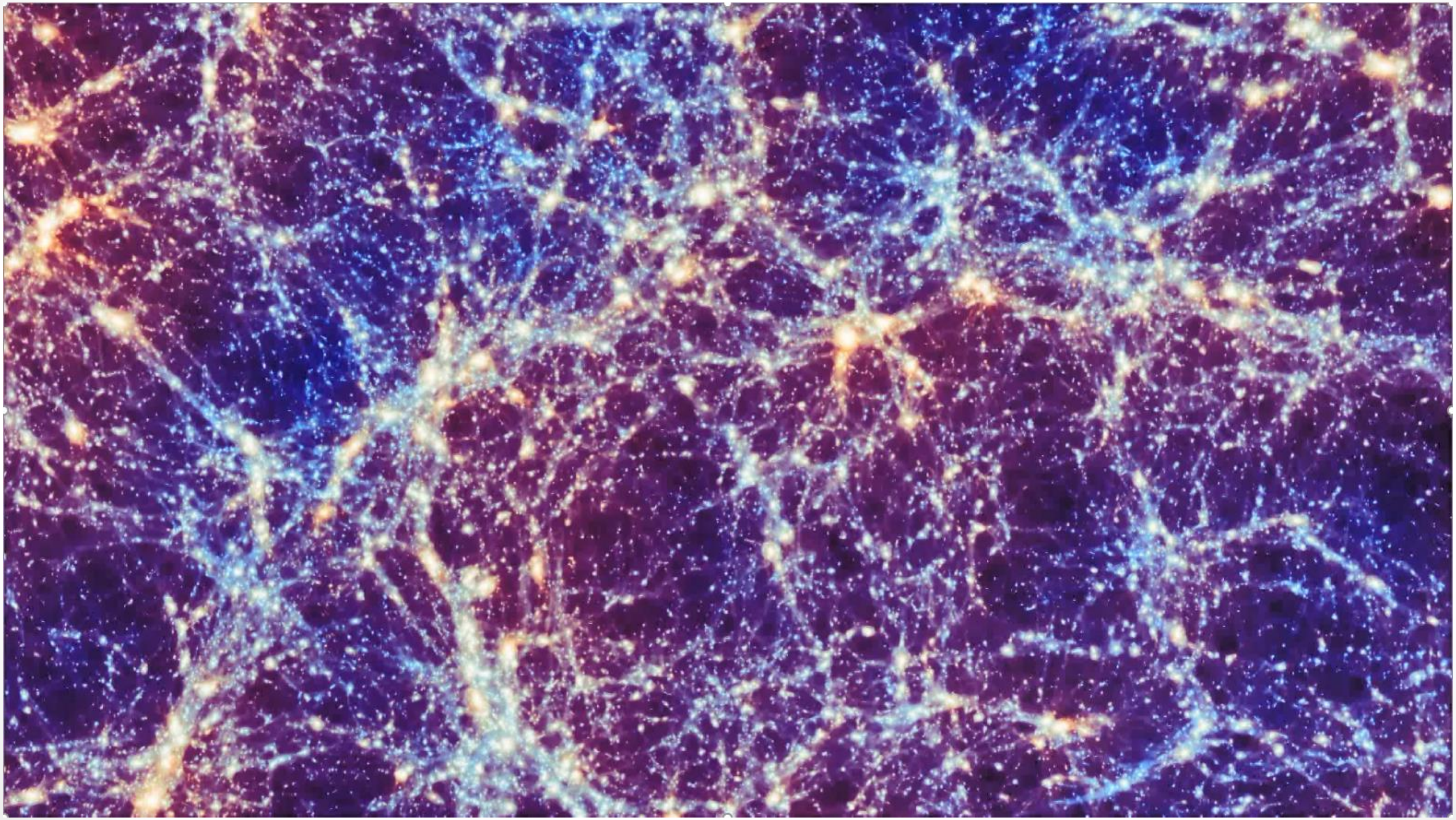

Y. Dubois & S. Colombi (IAP)

Cosmic web properties: insights from simulations

- Anisotropic structure:
  - Elongated filaments
  - Flattened sheets

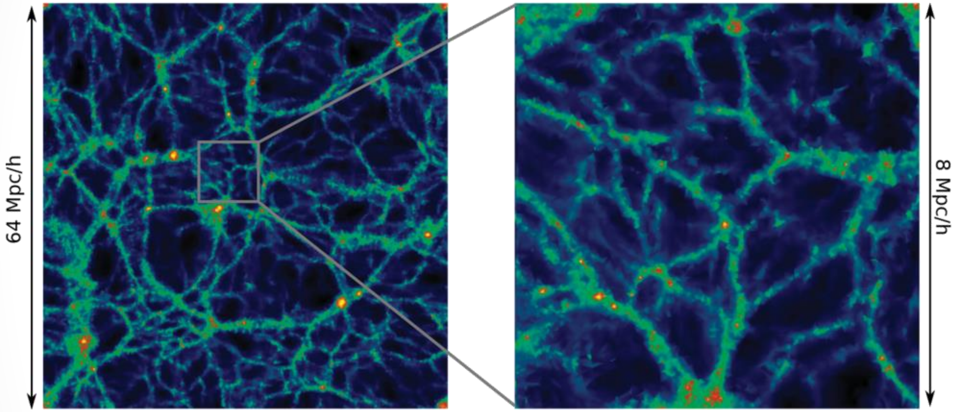

Aragon-Calvo & Szalay 2013, 1203.0248

- Multiscale/hierarchical nature:
  - Structures on a wide range of scales and density regimes
  - Overdense-underdense asymmetry

- Complex spatial connectivity:

Cosmic web

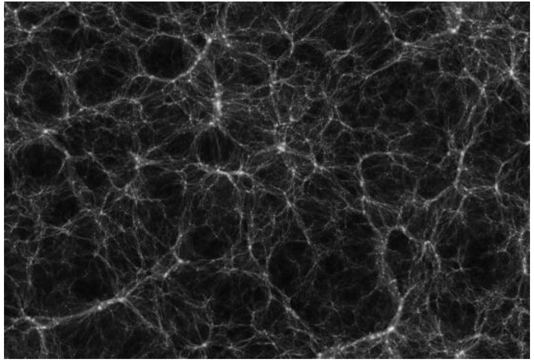

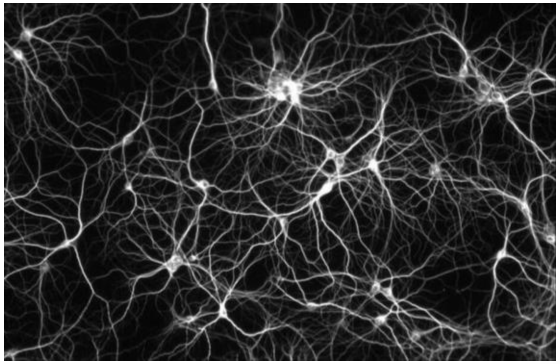

Human brain

Thermal cut-off in the linear power spectrum

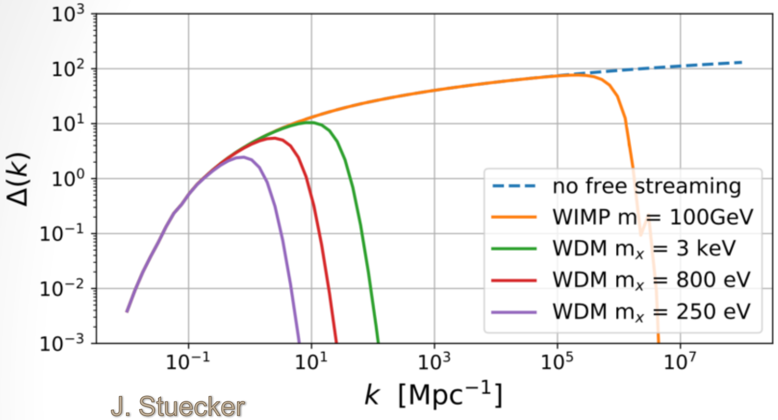

J. Stuecker

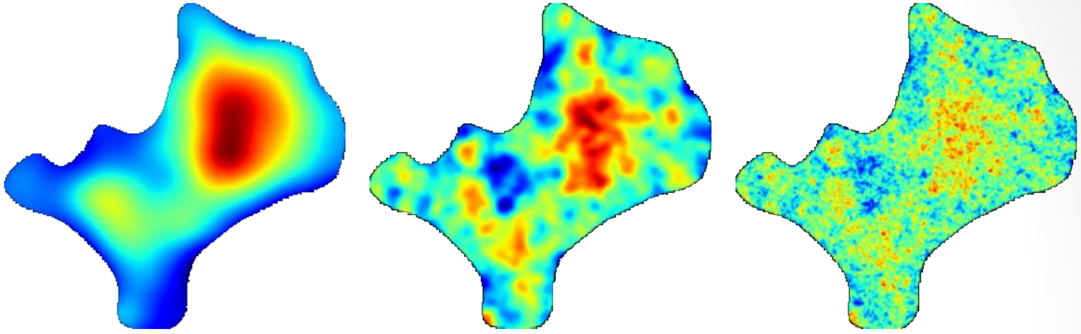

Neyrinck 2015, 1409.0057

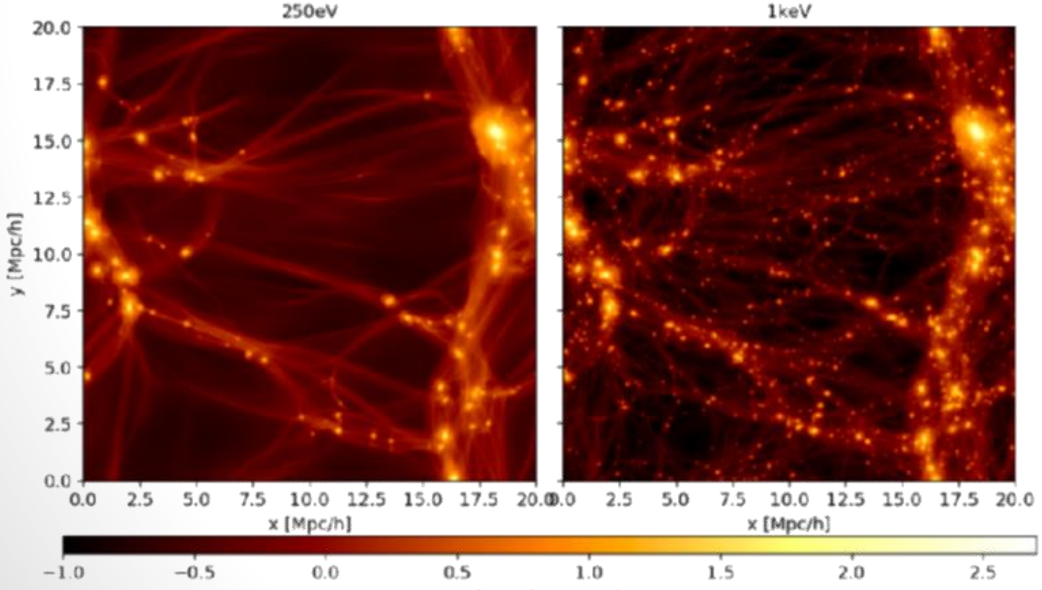

J. Stuecker

- The “CDM problem” (for simulators):

  halos down to Earth-mass scales in CDM!

Velocity field

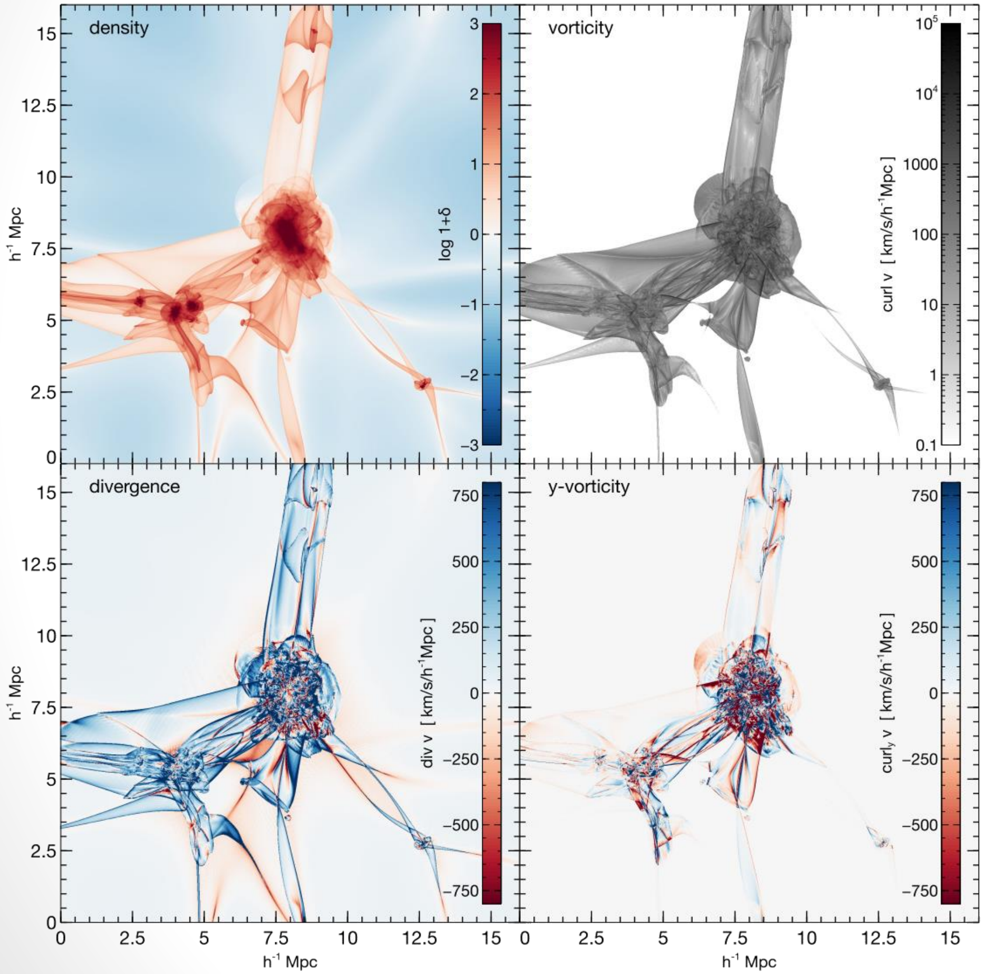

Hahn, Angulo & Abel 2015, 1404.2280

- At late times, shell-crossing breaks the trivial coupling between density and velocity divergence

- In the standard model, vorticity is a pure multi-stream phenomenon

Velocity dispersion

$\lambda_1 \geq \lambda_2 \geq \lambda_3$ eigenvalues of σ_{ij}

$$c_l \equiv (\lambda_1 - \lambda_2)/\left(\sum \lambda_i\right)$$

$$c_s \equiv 3\lambda_3/\left(\sum \lambda_i\right)$$

$$c_p \equiv 2(\lambda_2 - \lambda_3)/\left(\sum \lambda_i\right)$$

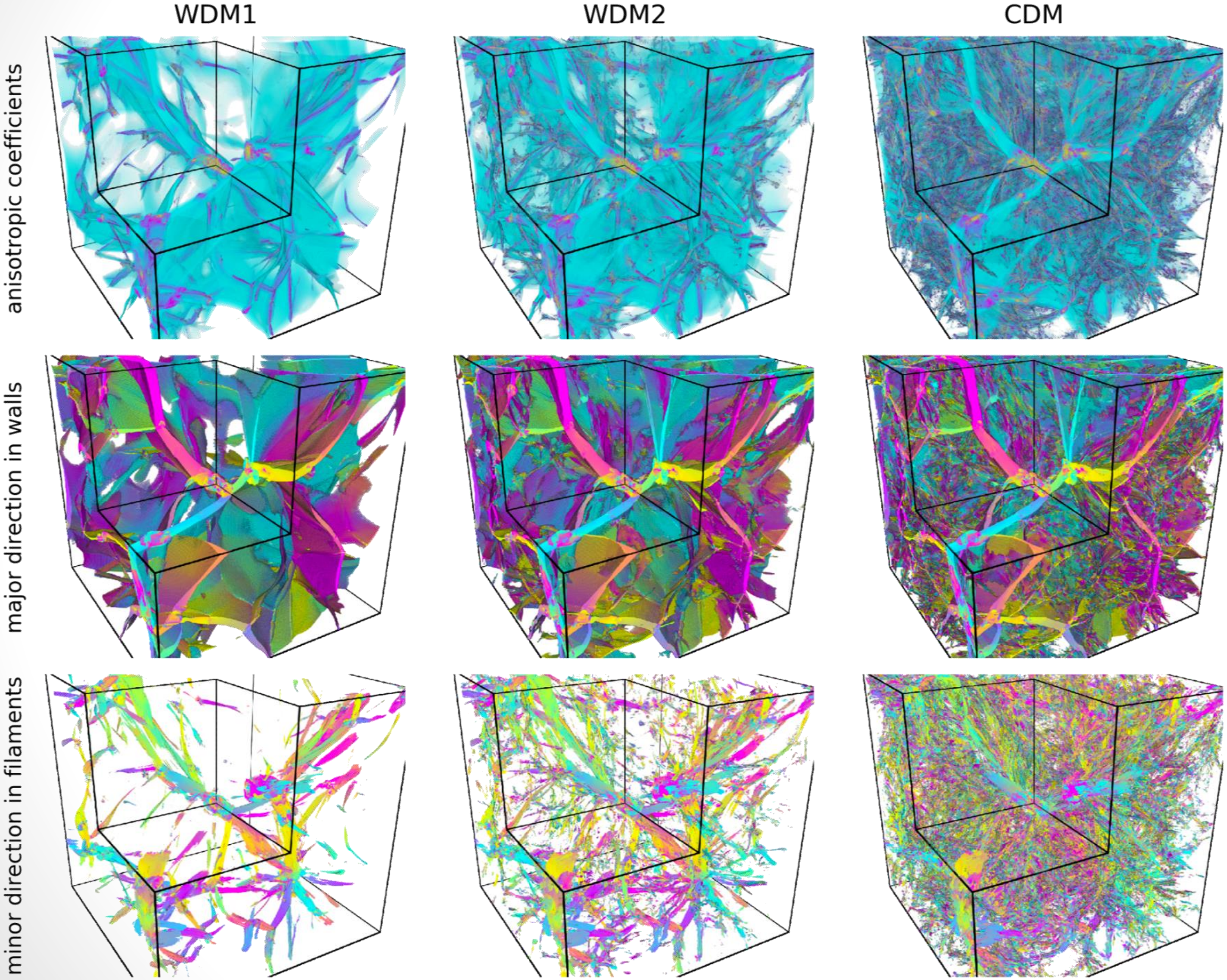

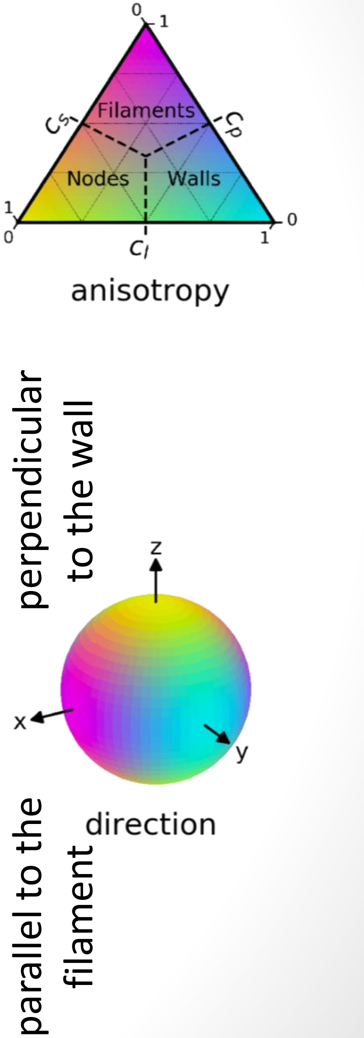

Buehlmann & Hahn 2019, 1812.07489

Observations

Where it all started…

- 1970-1980s: the structure formation controversy
  - Bottom-up scenario or “hierarchical clustering” (CDM): Peebles, Harrison, …
  - Top-down scenario or “adiabatic” (HDM): Zel’dovich, Arnol’d, …
- The discovery of voids in the galaxy distribution was initially met with scepticism… Until:

“A slice of the Universe”

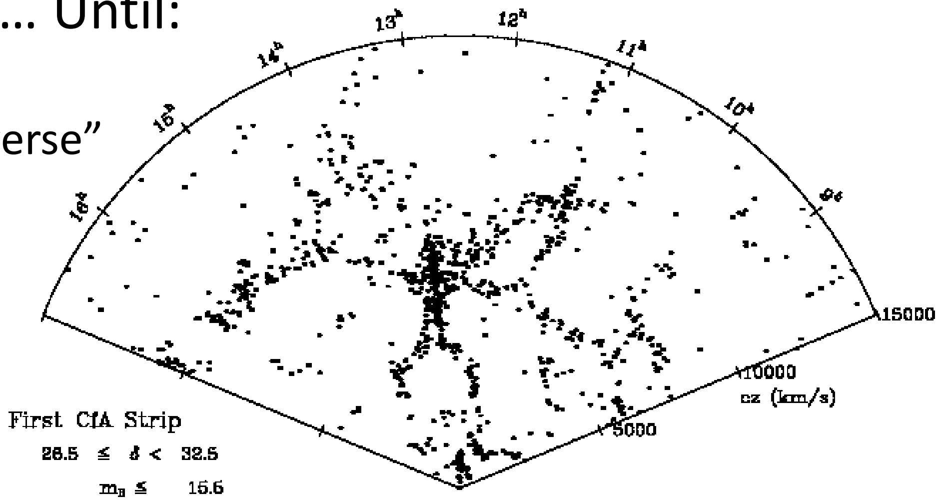

de Lapparent, Geller & Huchra 1986

- The “cosmic web theory” later solved the controversy

Bond, Kofman & Pogosyan 1995, astro-ph/9512141

2MASS (2003)

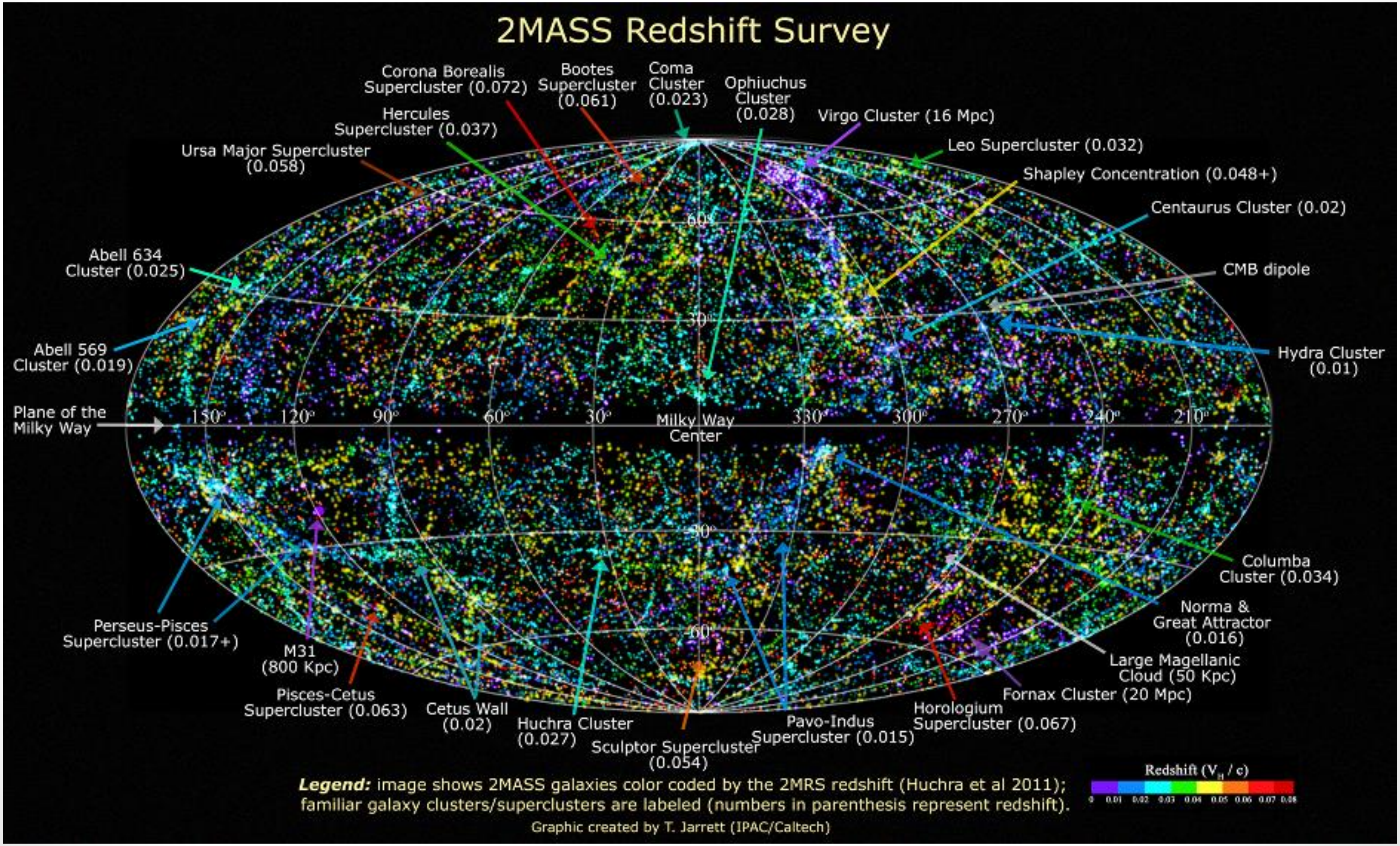
2MASS Redshift Survey
Corona Borealis Supercluster (0.072)
Bootes Supercluster (0.061)
Coma Cluster (0.023)
Ophiuchus Cluster (0.028)
Virgo Cluster (16 Mpc)
Hercules Supercluster (0.037)
Ursa Major Supercluster (0.058)
Leo Supercluster (0.032)
Shapley Concentration (0.048+)
Centaurus Cluster (0.02)
Abell 634 Cluster (0.025)
CMB dipole
Abell 569 Cluster (0.019)
Hydra Cluster (0.01)
Plane of the Milky Way
60°
30°
150°
120°
90°
60°
30°
Milky Way Center
330°
300°
270°
240°
210°
-30°
-60°
Columba Cluster (0.034)
Norma & Great Attractor (0.016)
Perseus-Pisces Supercluster (0.017+)
Large Magellanic Cloud (50 Kpc)
M31 (800 Kpc)
Fornax Cluster (20 Mpc)
Pisces-Cetus Supercluster (0.063)
Cetus Wall (0.02)
Huchra Cluster (0.027)
Sculptor Supercluster (0.054)
Pavo-Indus Supercluster (0.015)
Horologium Supercluster (0.067)
Legend: image shows 2MASS galaxies color coded by the 2MRS redshift (Huchra et al 2011); familiar galaxy clusters/superclusters are labeled (numbers in parenthesis represent redshift).
Redshift (V_H / c)
0
0.01
0.02
0.03
0.04
0.05
0.06
0.07
0.08
Graphic created by T. Jarrett (IPAC/Caltech)

Sloan Digital Sky Survey

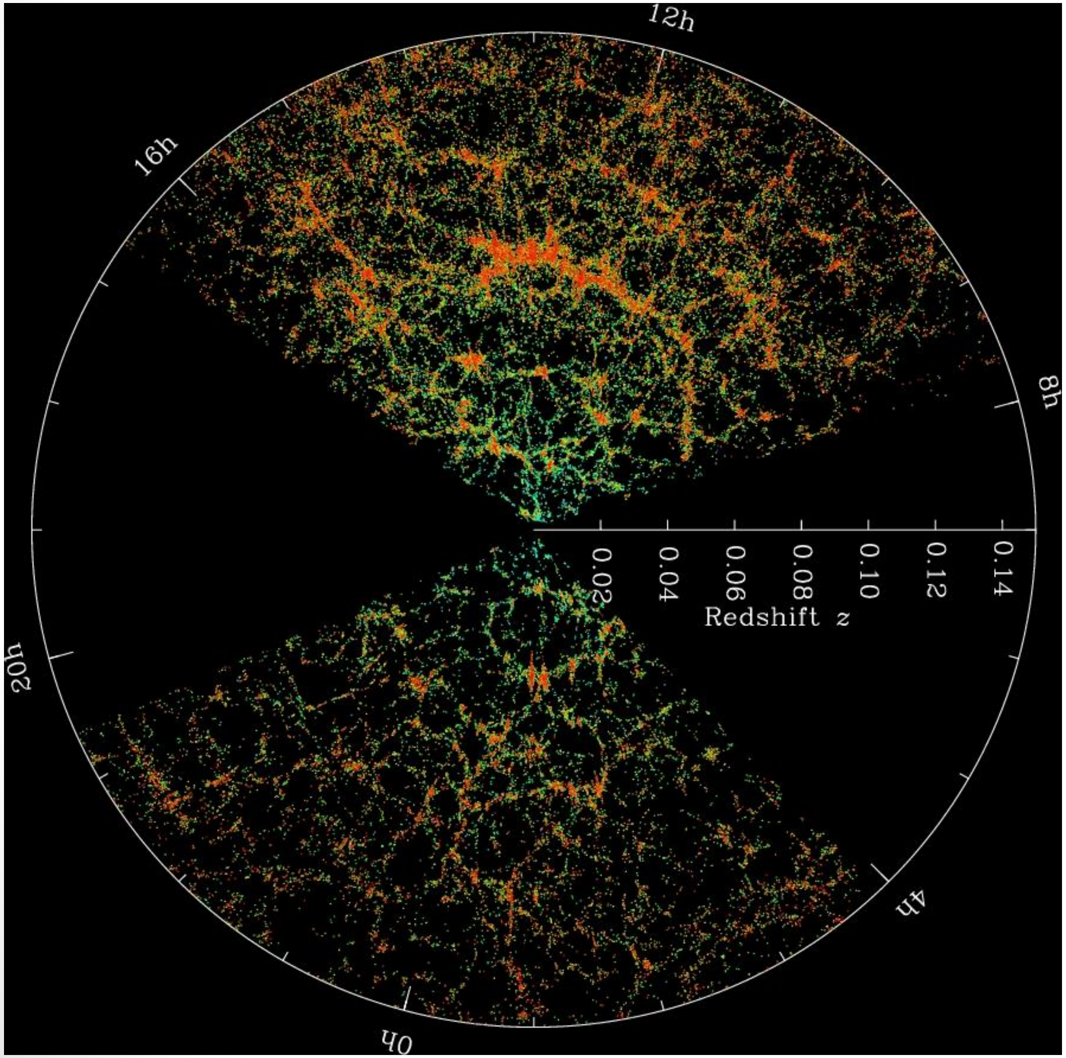

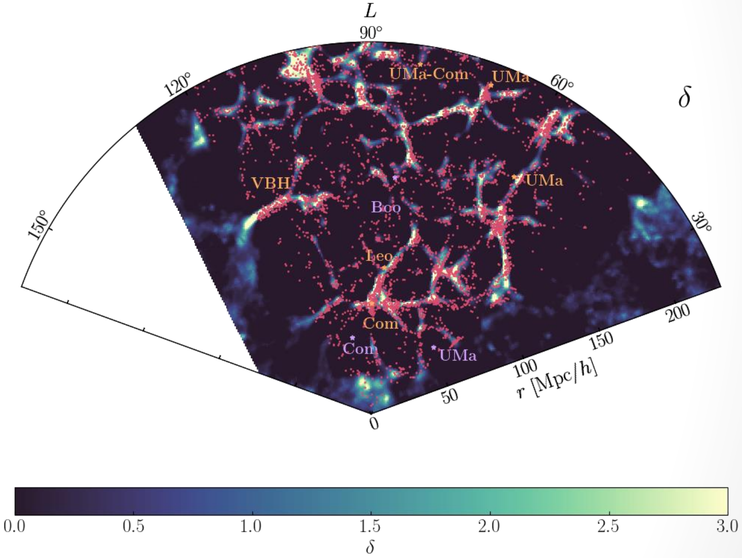

FL, Jasche, Lavaux, Wandelt & Percical 2017, 1601.00093

Large-scale structure surveys roadmap

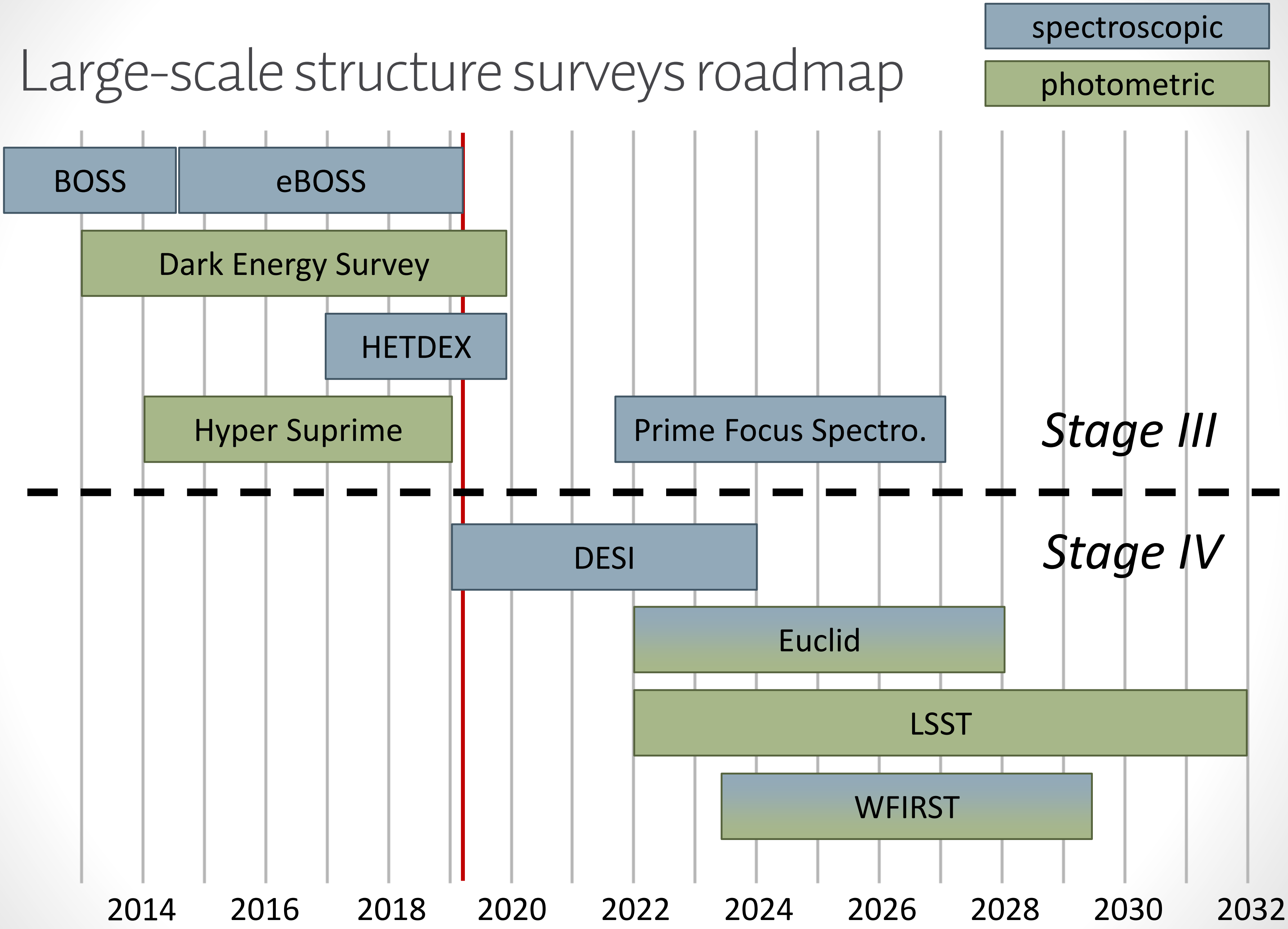

Reconstructions

The BORG inference framework

Bayesian Origin Reconstruction from Galaxies

- A Bayesian Hierarchical Model:

$\mathcal{P}(\hat{\delta}) \propto \exp\left(-\frac{1}{2}\sum_{k}\frac{\lvert\hat{\delta}_k\rvert^2}{P_k}\right)$	initial conditions
$\rho_\mathrm{m} = \mathcal{F}(\delta)$	total evolved matter density
$\rho_\mathrm{g} = \mathcal{B}(\rho_\mathrm{m})$	biased galaxy distribution
$\rho_\mathrm{g}^\mathrm{s}(\vec{x}) = S(\vec{x})\rho_\mathrm{g}(\vec{x})$	selected sample
$N_\mathrm{g} \curvearrowleft \mathcal{P}(N_\mathrm{g}\lvert\rho_\mathrm{g}^\mathrm{s})$	galaxy number count: random extraction (Poisson, Negative Binomial)

- The multi-million dimensional posterior distribution is sampled via Hamiltonian Monte Carlo.

Jasche & Wandelt 2013, 1203.3639 – Jasche, FL & Wandelt 2015, 1409.6308 – Lavaux & Jasche 2016, 1509.05040 – Jasche & Lavaux 2019, 1806.11117

The 2M++ galaxy compilation

Galaxy distribution

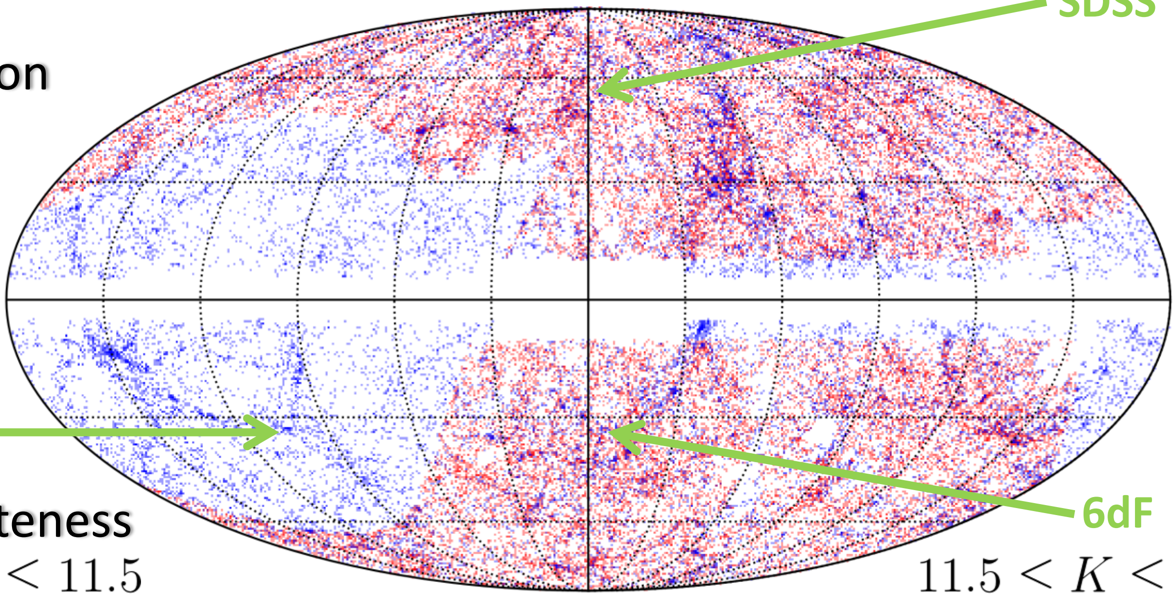

Redshift completeness

$K \leq 11.5$ $\quad$ $11.5 \leq K \leq 12.5$

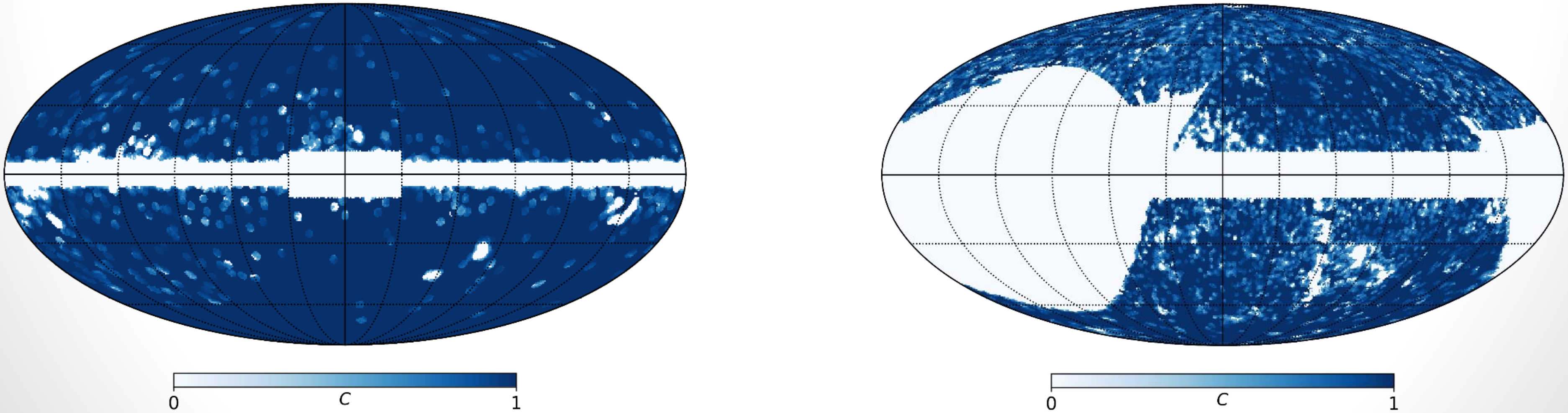

Lavaux & Hudson 2011, 1105.6107

BORG at work: Bayesian chrono-cosmography

Initial conditions **Final conditions** **Observations**

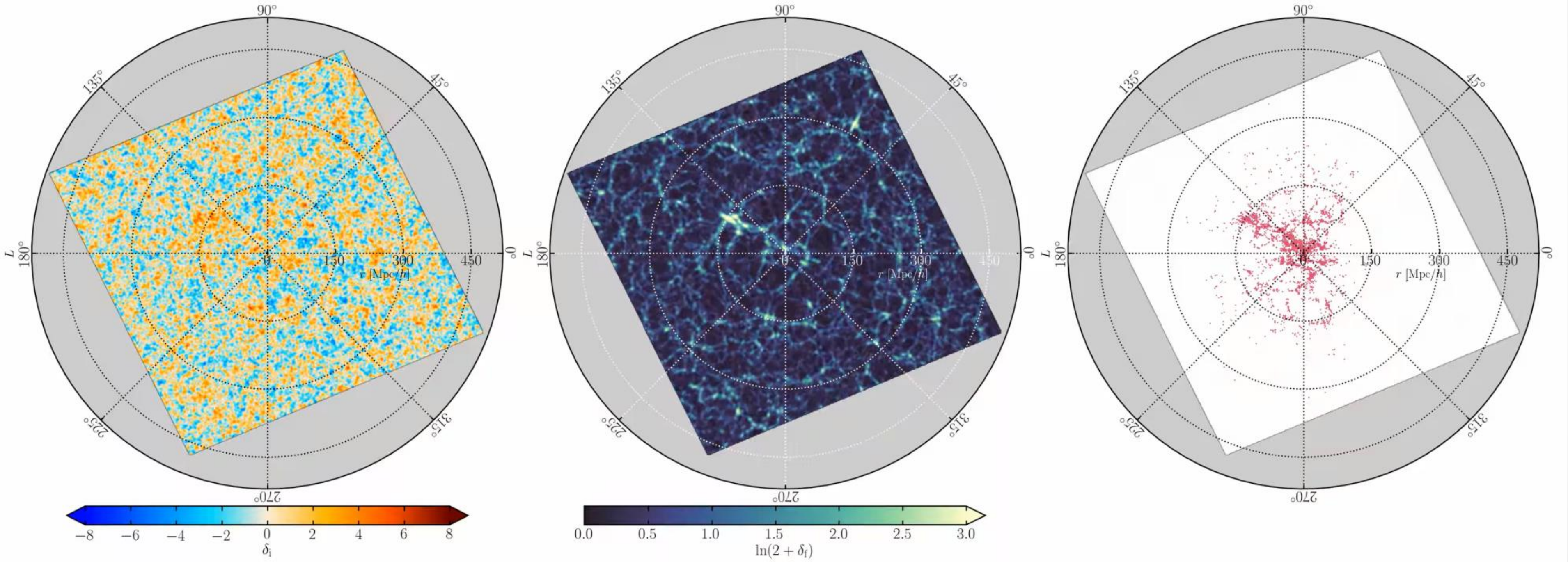

Supergalactic plane

67,224 galaxies, ≈ 17 million parameters, 5 TB of primary data products, 10,000 samples, ≈ 500,000 forward and adjoint data model evaluations, 1.5 million CPU-hours

Jasche & Lavaux 2019, 1806.11117

BORGPM density field: full non-linear dynamics

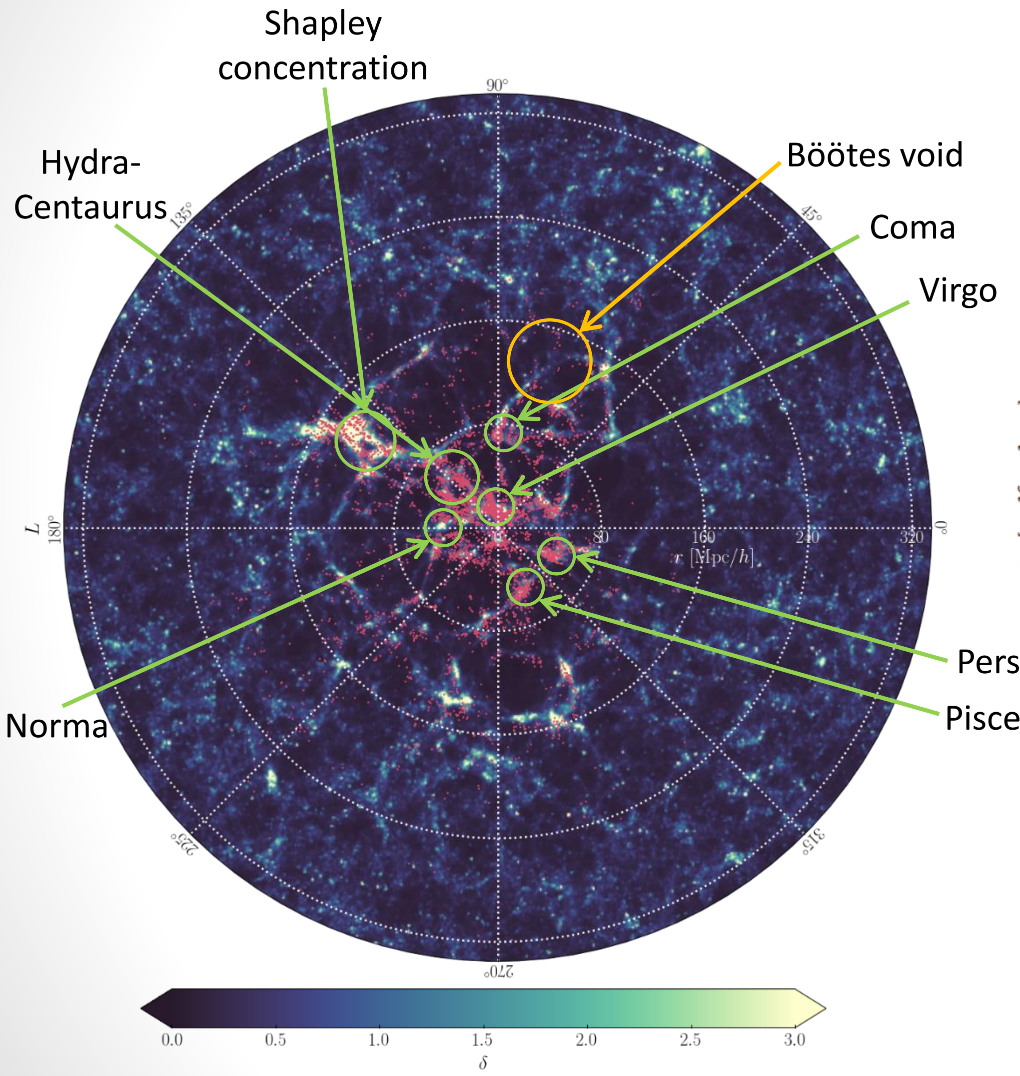

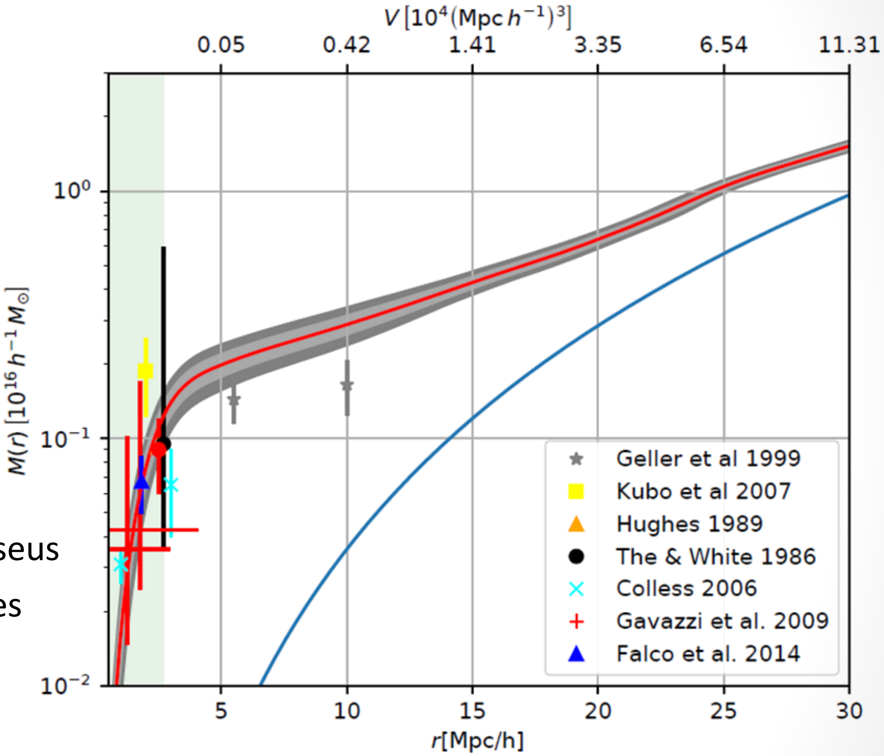

Mass profile of the Coma cluster, in agreement with gravitational lensing and X-ray observations down to a few Mpc.

Jasche & Lavaux 2019, 1806.11117 – FL, Lavaux & Jasche, in prep.

Velocity field in the supergalactic plane

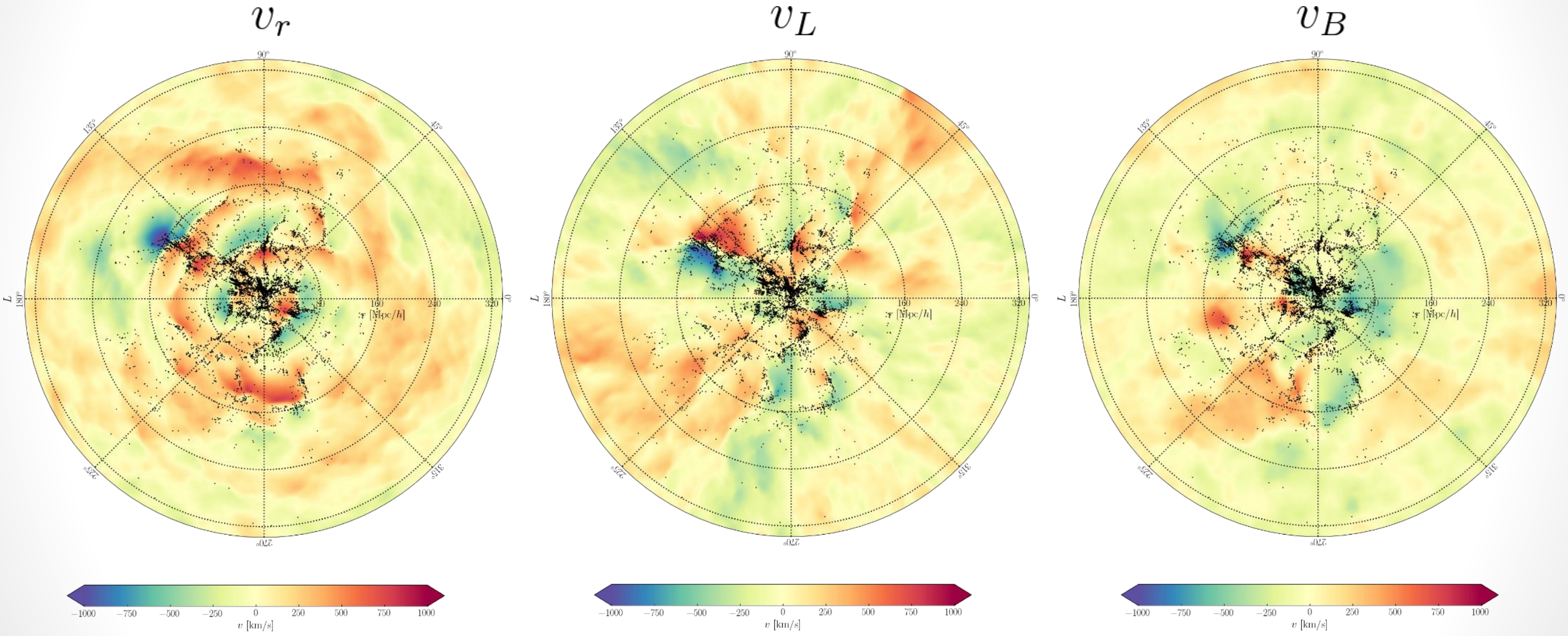

The gravitational infall of known structures can be observed.

FL, Lavaux & Jasche, in prep.

Number of streams and vorticity

Number of streams

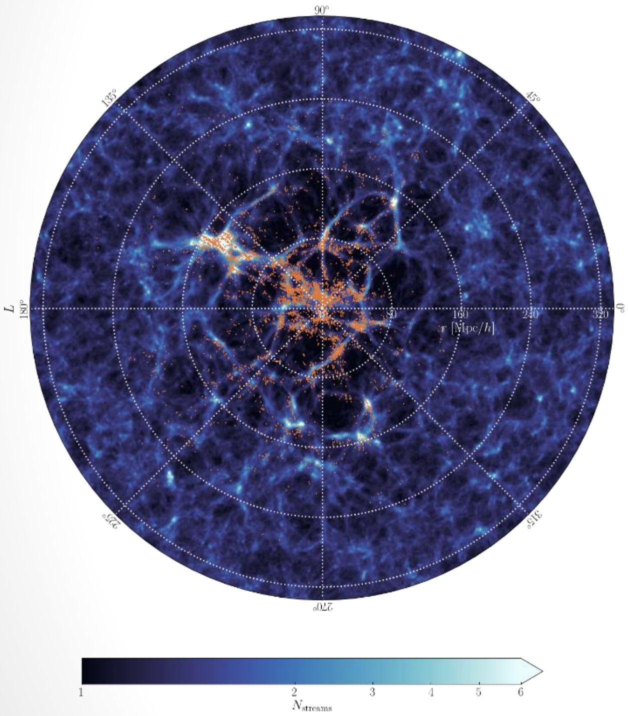

Velocity potential

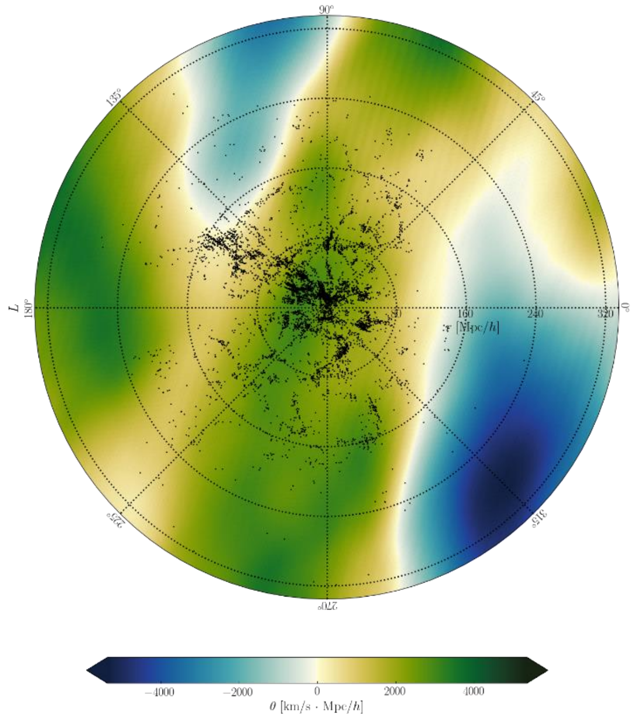

Norm of vorticity

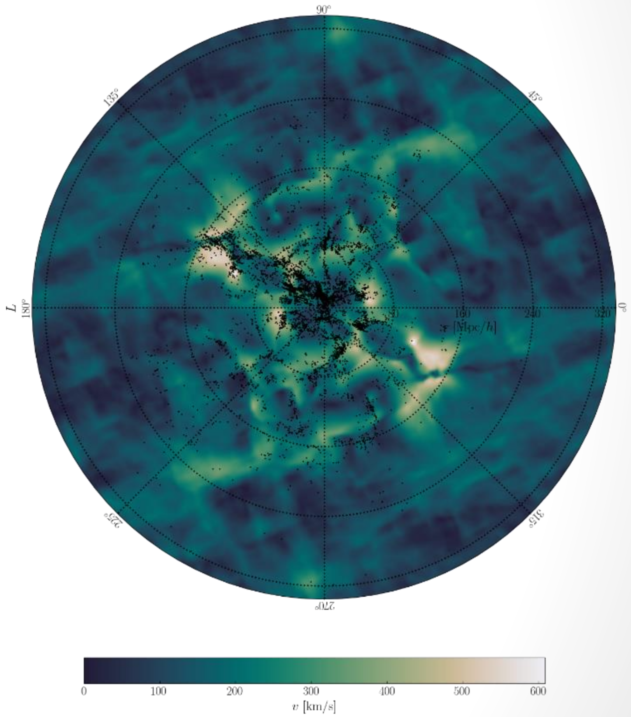

In earlier work (Leclercq, Jasche, Lavaux, Wandelt & Percival 2017, arXiv:1601.00093), these were postdictions. Thanks to BORGPM (full non-linear dynamics), we have now actual measurements - with uncertainties.

FL, Lavaux & Jasche, in prep.

Lagrangian Invariants Classification of Heterogeneous flows (LICH)

Lagrangian invariants

$$\mathcal{R}_{\ell m} \equiv \frac{\partial \Psi_\ell}{\partial \mathbf{q}_m} \qquad \lambda^3 + \boxed{s_1}\lambda^2 + \boxed{s_2}\lambda + \boxed{s_3} = 0$$

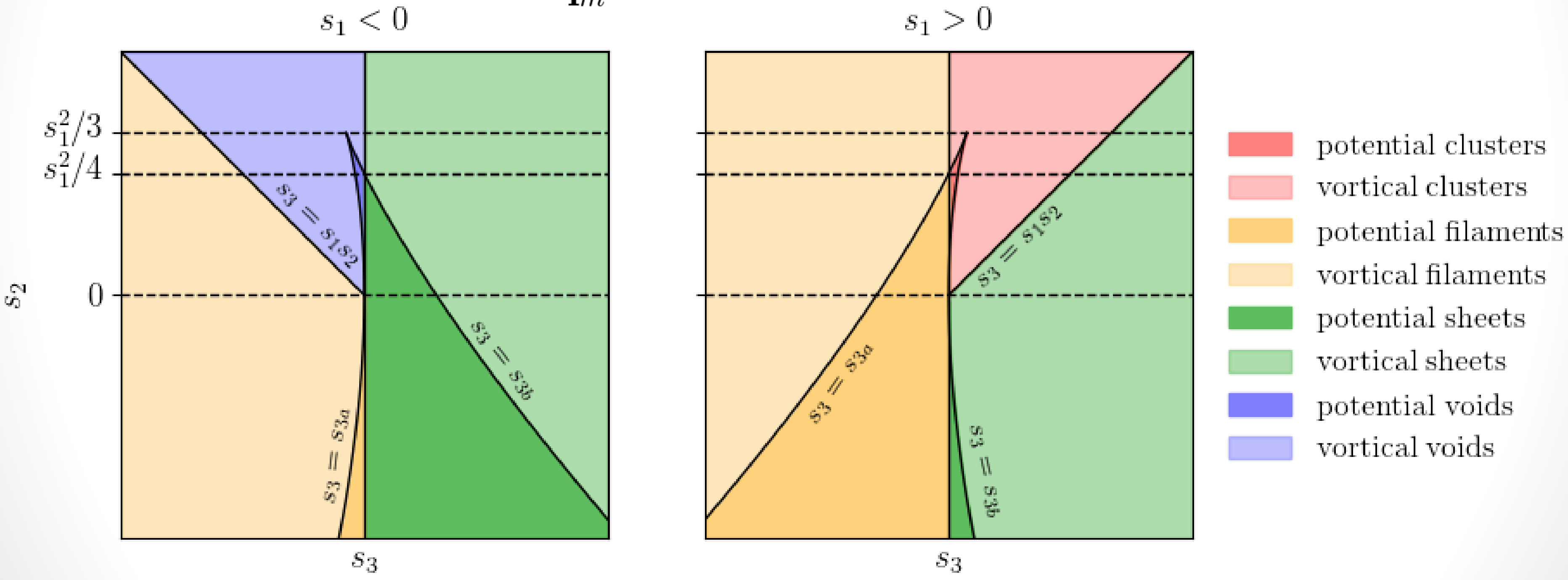

FL, Jasche, Lavaux, Wandelt & Percival 2017, 1601.00093

Generalises DIVA,

Lavaux & Wandelt 2010, 0906.4101

LICH initial structures inferred by BORG

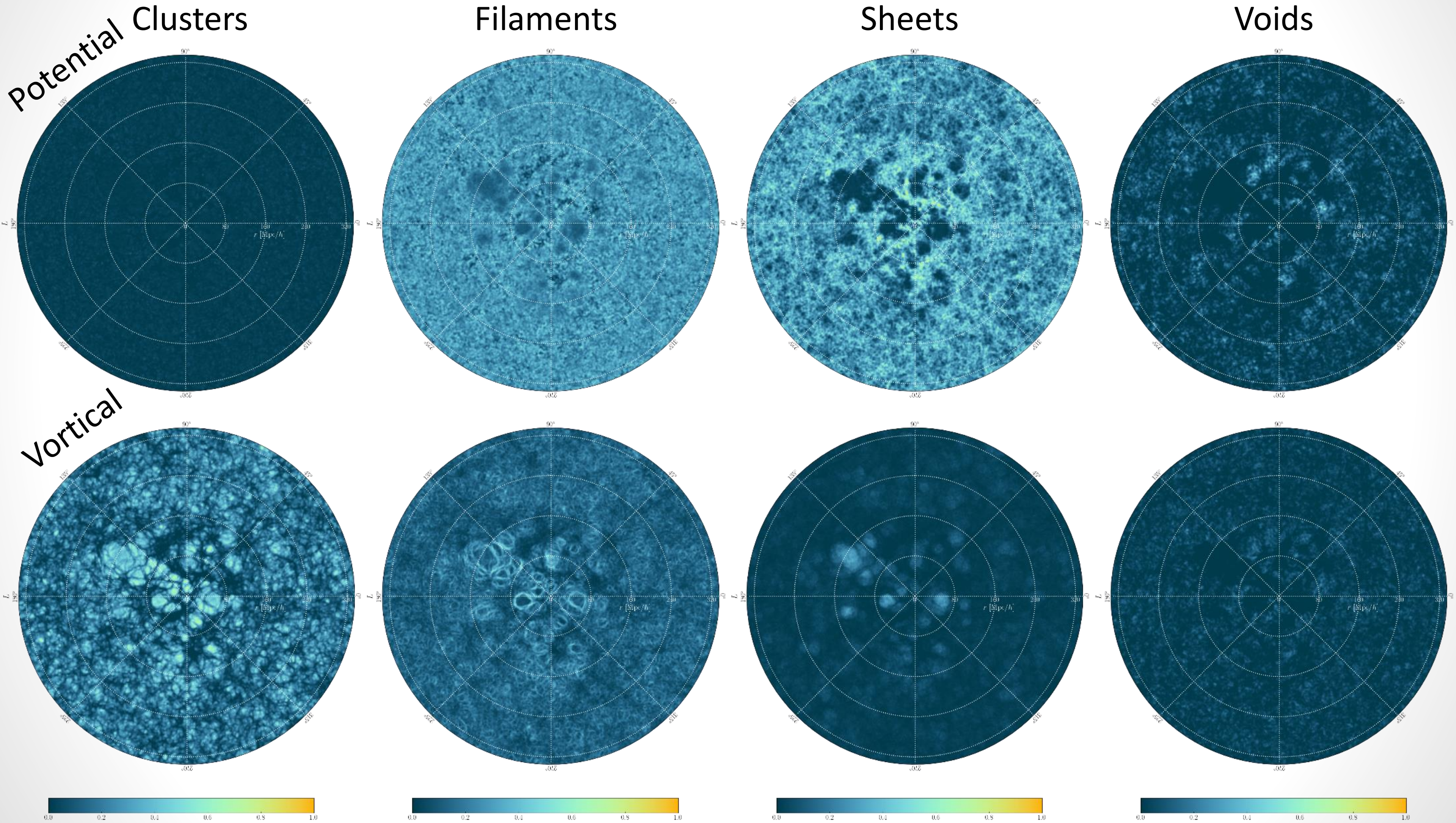

Clusters

Filaments

Sheets

Voids

Potential

Vortical

FL, Lavaux & Jasche, in prep.

LICH final structures inferred by BORG

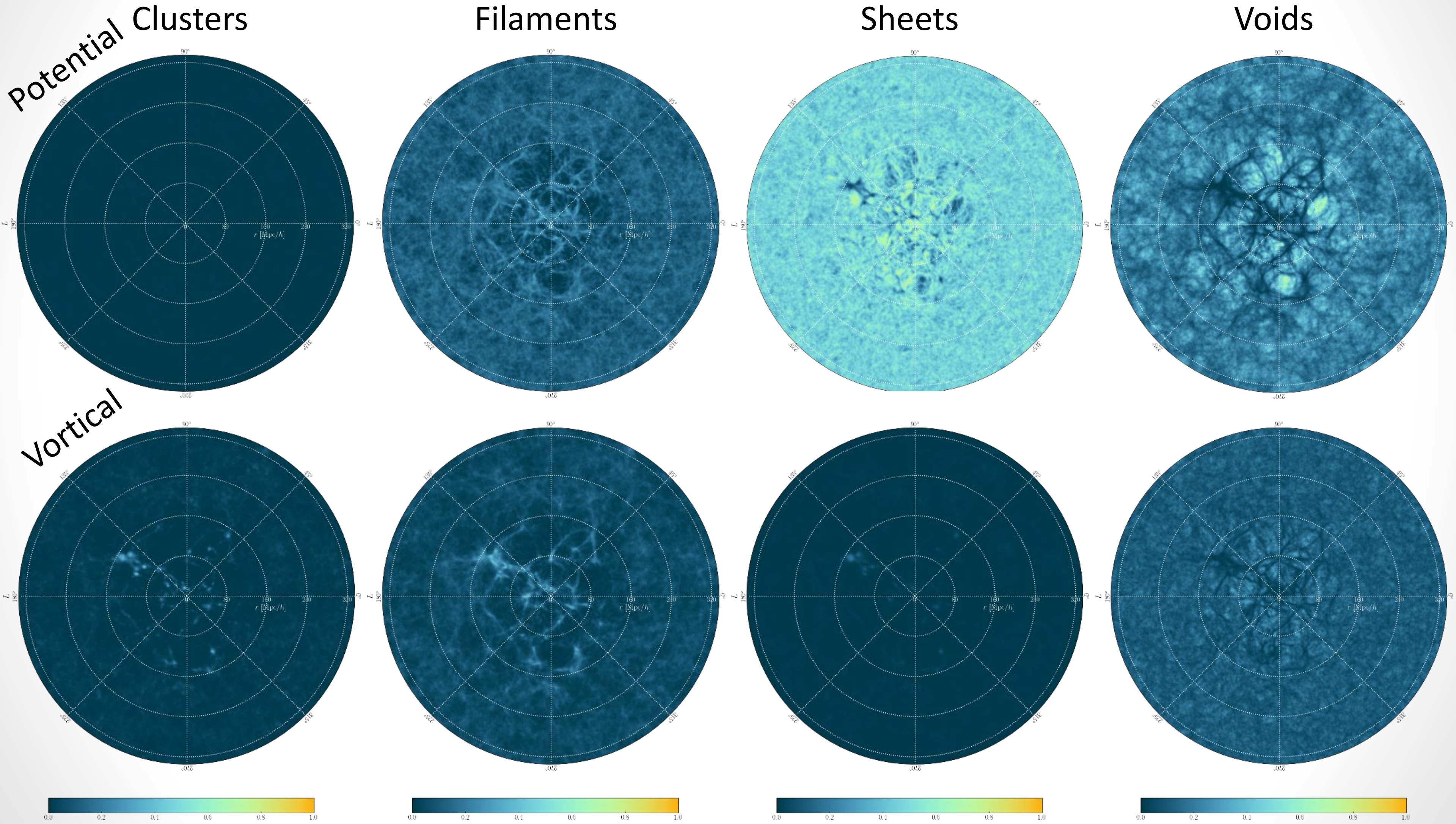

Clusters

Filaments

Sheets

Voids

Potential

Vortical

FL, Lavaux & Jasche, in prep.

Mapping the Universe: epilogue?

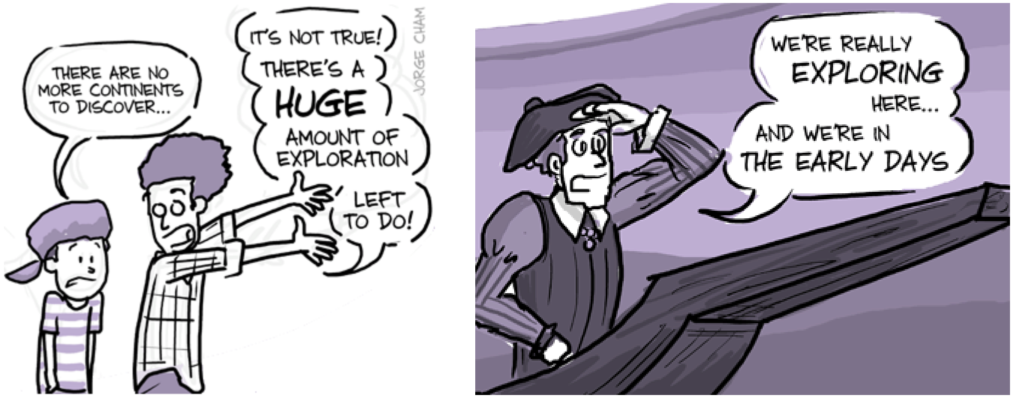

J. Cham – PhD comics